POLITECNICO
MILANO 1863

SCUOLA DI INGEGNERIA INDUSTRIALE
E DELL'INFORMAZIONE

Executive Summary of the Thesis

# Aeroacoustic characterization of a 3D organ pipe

Laurea Magistrale in Aeronautical Engineering - Ingegneria Aeronautica

**Author:** Óscar Martínez Díaz

**Advisor:** Prof. Paolo Schito

**Co-advisor:** Alberto Artoni

**Academic year:** 2021-2022

## 1. Introduction

A fascinating field in which aeroacoustic can provide more insight on the physical mechanism of sound generation and propagation is musical acoustics. The air flow in musical instruments is a long standing problem in the field of musical acoustics due to the essential non-linearity of the governing equations.

Flue instruments are wind instruments in which sound is produced by flow instability without significant wall vibration, and hence the wall can be considered rigid. In organ pipes the flow instability comes from an air jet impinging a sharp edge. This creates an acoustical excitation that then propagates inside the organ pipe, which acts as an acoustic resonator.

To best understand the sound generation and propagation mechanism, it was decided to study the process through its fluid dynamics, using the traditional tools this field provides together with those contributed by the field of aeroacoustics.

The final goal of this work is to study and validate the methodology to correctly perform a three-dimensional computational experiment of the turbulent fluid flow and the coupled acoustic field created by a flue pipe musical instrument, particularly an organ pipe. The main reference for this work are those developed by Fischer *et al.* [1], in which a two-dimensional computational simulation of the fluid flow around a organ pipe was compared with experimental results.

The thesis is organised as follows. In Section 2, the methodology used is briefly explained. Section 3 consists of all the numerical results obtained, starting with the validation of the methodology through a simple aeroacoustic case, namely the laminar flow around a squared cylinder in Subsection 3.1. Next in Subsection 3.2, we simulate the flow of a two-dimensional organ pipe, with comparison of the results to those obtained by Fischer *et al.* [1]. We then consider in Subsection 3.4 the final three-dimensional organ pipe model, where we employ the same modelling and numerical strategy of the two-dimensional case. Comparisons between the cases and to experiments are made to extract some validation and differences between the cases. Finally, Section 4 finishes the thesis with a summary and the conclusions obtained from the obtained results.

## 2. Methodology

The results are obtained using the OpenFOAM software, solving the compressible Navier-Stokes equations. In the first considered test case, a direct noise computation was performed on a lam-

$$\left.\begin{aligned} \tau_{ij} &= -2\nu_{SGS}\overline{S}_{ij} + \frac{2}{3}\delta_{ij}k_{SGS}\,, \\ \nu_{SGS} &= C_k k_{SGS}^{1/2}\Delta \\ -\rho\tau_{ij} : \overline{D}_{ij} - C_\epsilon\frac{\rho k_{SGS}^{3/2}}{\Delta} &= \frac{\partial(\rho k_{SGS})}{\partial t} + \frac{\partial(\rho\overline{u}_j k_{SGS})}{\partial x_j} - \frac{\partial}{\partial x_j}\left[\rho(\nu+\nu_{SGS})\frac{\partial k_{SGS}}{\partial x_j}\right] \end{aligned}\right\} \quad (1)$$

inar square cylinder. The following test cases the turbulence is modelled by employing LES turbulence with the one-equation model for the kinetic energy shown in Equation 1 [2].
To deal with the far field acoustic field, the Ffowcs Williams and Hawkings aeroacoustic analogy was chosen. Particularly, in this thesis, aeroacustics of the far field are computed using the third-party open-source library `libAcoustics` of OpenFOAM, which bases its computation in the Farassat's Formulation 1A of the Ffowcs Williams and Hawkings aeroacoustic analogy. The equation that computes the fluctuating pressure is shown in Equation 2.

## 3. Numerical Results

The aim of this thesis is to provide an understanding of the computational aeroacoustics obtained using OpenFOAM in different cases of increasing complexity, studying the sound emission and propagation.

### 3.1. Square Cylinder

The first case studied in this thesis is the flow around a square cylinder. The results were validated using the DNS performed by Inoue *et al.* [3]. The computational domain for this case is an O-grid with a radius of $150D$, with $D$ being the size of the cylinder. The studied problem is represented by a rigid square cylinder immersed in a compressible, unsteady, laminar flow of Mach number $Ma = 0.2$, with a Reynolds number of $Re = 150$, and a Prandtl number of $Pr = 0.75$. The fluid is considered a perfect gas $\rho = p/(RT)$. The simulation is carried on using the solver `rhoCentralFoam` for a non-dimensional computational time of $TU_\infty/D \approx 400$, using a non dimensional time step of $\Delta t U_\infty/D \approx 2\times10^{-4}$ to keep the CFL number under 1.
Table 1 lists different results obtained and their comparison with the literature. The obtained results match the reference obtained from Inoue *et al.* Also the peaks $\Delta C_l$ and $\Delta C_d$ - that are crucial to match the noise intensity since they indicate the strength of the sound source - match the reference.

| | **Results** | **Inoue *et al.* [3]** |
|---|---|---|
| $St$ | 0.150 | 0.1512 |
| $C_{d,mean}$ | 1.4850 | 1.414 |
| $\Delta C_d$ | 0.0207 | 0.0204 |
| $C_{l,mean}$ | -0.0083 | 0 |
| $\Delta C_l$ | 0.4063 | 0.3923 |

Table 1

A polar plot containing the root mean square of the fluctuating pressure $p_{rms}$ is shown to investigate the nature of the sound in the far field. Specifically, this pressure directivities are shown in Figure 1, with data collected from a total of 64 probes positioned on the flow field, equally separated on the polar coordinate at a radius of $75D$ from the centre of the square cylinder. As comparison, it also shows the results obtained from a DNS and from an experiment using Curle's aeroacoustic analogy. The results of Inoue *et al.* have a directivity of 95°, where for the obtained results it is located at 99.7°. It is clear that this approach ensures a good reconstruction of the acoustic far field, with a difference in the direction of the maximum sound pressure level of less than 5°. The directivity pattern is that of a dipole, meaning that the main sound source is given by the forces acting on the cylinder, with only a slight overshoot of the sound intensity with respect to the DNS. This was expected since in the computed results the peaks are slightly higher. The small deviation in the upstream between the results from Ali *et al.* is due to the Doppler effect (taken in the moving frame), which is not taken into account in that study.

$$4\pi p'(\mathbf{x},t) = \int_{f=0}\left[\frac{\rho_0 \dot{u}_n}{r(1-M_r)^2} + \frac{\rho u_n \hat{r}_i \dot{M}_i}{r(1-M_r)^3}\right]_{ret} d\Sigma + \int_{f=0}\left[\frac{\rho_0\, c\, u_n (M_r - M^2)}{r^2(1-M_r)^3}\right]_{ret} d\Sigma +$$
$$\int_{f=0}\left[\frac{\dot{p}\cos\theta}{cr(1-M_r)^2} + \frac{\hat{r}_i \dot{M}_i p \cos\theta}{cr(1-M_r)^3}\right]_{ret} d\Sigma + \int_{f=0}\left[\frac{p(\cos\theta - M_i n_i)}{r^2(1-M_r)^2} + \frac{(M_r - M^2)p\cos\theta}{r^2(1-M_r)^3}\right]_{ret} d\Sigma \quad (2)$$

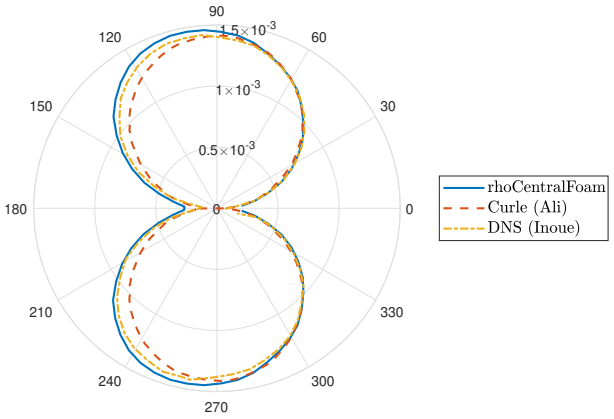


Figure 1

### 3.2. Two-dimensional organ pipe

In this section, the flow inside an organ pipe is considered. The geometry of the organ pipe was obtained from the study performed by Fischer *et al.* [1]. Particularly, the two-dimensional computational grid consists of an inlet of 0.6 mm with a distance of 5.5 mm between itself and the leading edge of the resonator. This last part has a length of 106 mm and a height of 9.5 mm. The resonator has solid walls of 6 mm of width. The computational domain is contained in a rectangle of 260 × 180 mm.

Initially, the flow is static, with an initial pressure of $p_0 = 101325$ Pa, a temperature of $T_0 = 293$ K, a kinematic viscosity of $\nu = 1.53 \cdot 10^{-5}$ $m^2/s$. From the inlet, the flow is expelled with a velocity of 18 m/s, corresponding to a Mach number of $Ma \approx 0.052$, in a direction parallel to the resonator. The reference length for this problem is assumed to be the distance between the inlet and the leading edge, regarding to the free propagation length of the jet. The fluid is considered a perfect gas $\rho = p/(RT)$. The simulation lasts for 100 ms, that is enough simulation time to obtain statistically significant results for the flow.

With this values the Reynolds number is estimated as $Re \approx 6470$ and a Prandtl number of $Pr = 0.72$. For the considered regime, we expect a weak turbulence behaviour. The vortex shedding frequency in the mouth region is caused by the oscillations of the jet. The hypothesis is that the vortex shedding frequency will synchronise with the resonator and correspond to the fundamental frequency of the real operating organ pipe $f = 700$ Hz. The Strouhal-number is estimated at $St \approx 0.214$.

Figure 2 shows the geometry of the model and the initial wave travelling through the resonator. The travelling speed of this planar wave can be estimated as 341 m/s.

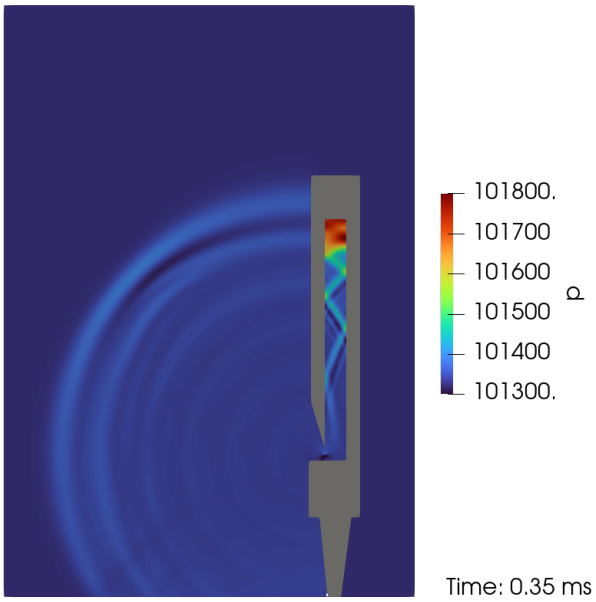


Figure 2

Figure 3 shows the instantaneous velocity field obtained at $t = 100$ ms. In an organ pipe, the jet of air impinges against the leading edge of the tube and generates vortices, as seen here, which creates the sound defined as the edge tone. This couples with the acoustic resonance that turns small perturbations into periodic oscillations with large amplitudes that occurs in the resonator (Figure 2), called the pipe tone. The edge tone is weaker and shorter in duration than the pipe tone. The edge tone jet initiates the subsequent pipe tone and pairs with it produc-

ing a louder, more harmonically rich, and more stable audible sound.

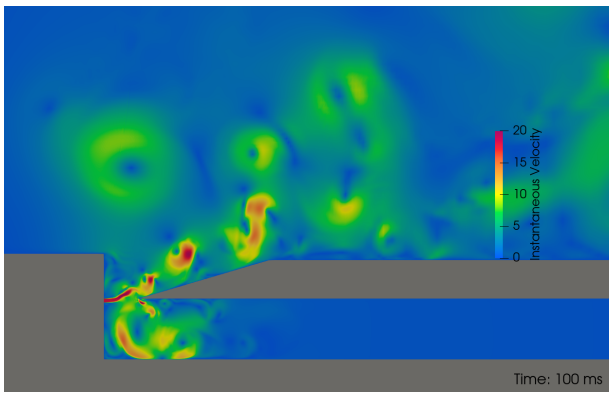


Figure 3

Following the procedure of Fischer *et al.*, Figure 4 shows the spatially averaged SPL obtained over the exit of the organ pipe's mouth. Labeled are the peaks of the acoustic pipe mode frequencies (1st, 3rd and 5th), but also the even (2nd, 4th and 6th) harmonics for the closed end pipe. The deviation of the experimental data is only of 5% in frequency. The experimental data was obtained using a microphone separated by 0.5 m from the mouth area and the data has also offseted, which explains the difference in the values of the amplitude.

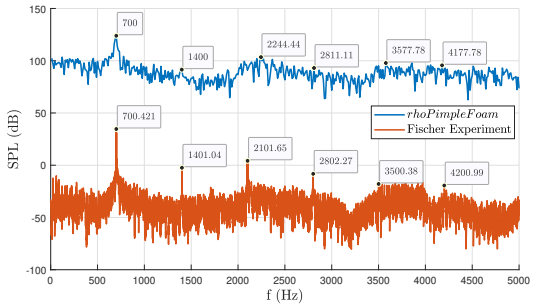


Figure 4

A computation of the fluctuating pressure outside of the computational domain using the FWH acoustic analogy was also performed. Figure 5 shows the SPL obtained through a probe situated inside the computational domain, and an through FHW suing an observer outside the computational domain.The FHW observer registers a lower amplitude with respect to the far field probe because it is positioned further away from the mouth of the instrument. The shape of the SPL is similar between both results, with similar valleys and peaks, with a more notable peak on the second harmonic (∼ 1400 Hz) on the FWH observer compared with the probe.

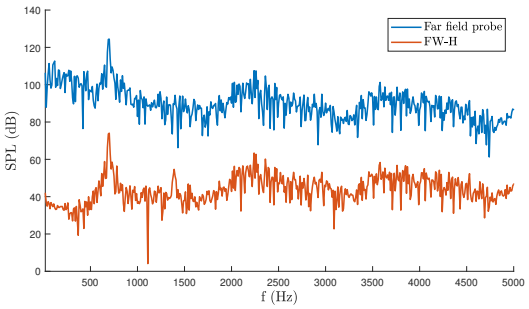


Figure 5

### 3.3. Parametrical study of 2D organ pipe geometry

Following the study and validation of the standard geometry, another set of simulations were performed modifying the geometry of the organ pipe. Specifically, the position of the leading edge was changed. The objective of this section is to observe the change in behaviour of the aeroacoustic flow when this condition is altered. The different geometries studied were created by moving the leading edge of the resonator. Figure 6 shows the different configurations studied: In blue, the positioning of the standard organ pipe, the only object of study until this point. Red marks the geometry of the close edge. The next edge considered, marked in yellow, is called the far edge. Finally, purple marks the furthest edge geometry.

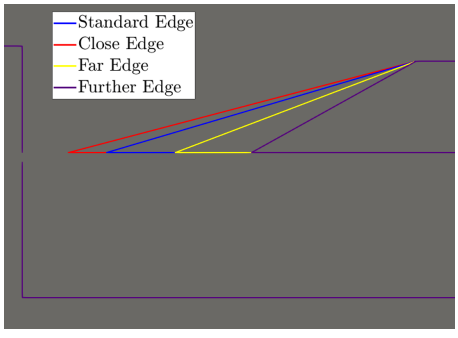


Figure 6

Figure 7 shows the SPL-spectrum of the different leading edge configurations. Compared to the reference configuration, the close leading edge has the first harmonic on a lower frequency. Moving the edge closer to the inlet, makes the

actual length of the resonator longer, and therefore the frequency of the first harmonic is the smaller of all the configurations. Conversely, when the position of the leading edge is pushed away from the inlet, the resonator is effectively shorter and therefore register a higher frequency for the first harmonic.
Another behaviour of organ pipes can be found here. Similar to the edge tone (first hydrodynamic mode), for lower values of the jet velocity there is a proportional relation with the frequency of produced by the instrument. When the latter reaches the value of the fundamental frequency of the pipe, synchronisation happens. The recorded frequency is locked to the this fundamental frequency until the edge tone frequency is close to the third harmonic, and as closed pipes only develop odd harmonics it works as the second acoustic pipe mode frequency. This second synchronisation causes a jump in the registered frequency to the second resonance.
This phenomenon happens on the organ pipe configuration with the close leading edge of the resonator. As the edge is closer, the second acoustic pipe mode is reached with a lower jet velocity than the standard case. For this reason, on Figure 7 it can be seen how the dominant frequency for the close edge case is the third harmonic.

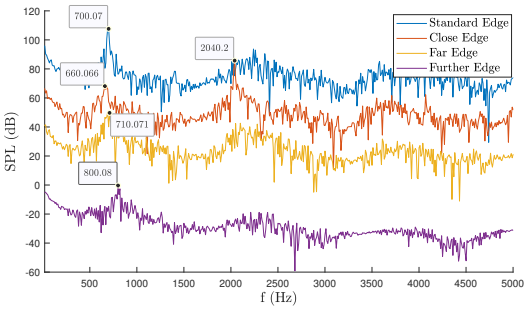


Figure 7

## 3.4. Three-dimensional organ pipe

The studied flow follows the same structure as the two-dimensional case, maintaining the same dimensions and adding 9.5 mm of with to both the resonator and the inlet. For the flow, the same physical magnitudes are used. The computational domain is contained in a prism of $125 \times 36.5 \times 51.5$ mm.

The mesh for the three-dimensional case is created using the two-dimensional case as a reference. The centre of the mesh, which covers the entirety of the resonator, is an extrusion of the two-dimensional case. For this, a total of $6.4416 \times 10^6$ cells where employed, more than 50 times those used for the previous case.
The main drawback of performing a computational three-dimensional experiment is the increased computational cost with respect to the two-dimensional case. The three-dimensional mesh has over 50 times the number of cells. The numerical simulations were calculated in parallel on the computational cluster of the Department of Mechanical Engineering of Politecnico di Milano, using 4 computational cores for the two-dimensional case and 40 cores for the three-dimensional case. As a result, the time needed to computationally simulate the 100 ms of each case goes from approximately 28 hours in the two-dimensional case, to over 31 days on the three-dimensional case.
Figure 8 shows the pressure contours inside the three-dimensional model at the same time as Figure 2. A similar wave structure can be seen on both cases, with approximately the same travelling speed.

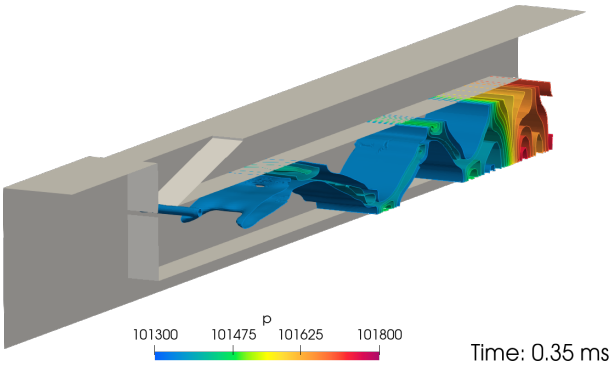


Figure 8

Figure 9 shows the time history of the pressure obtained by a probe positioned near the mouth. The three-dimensional case shows a smaller amplitude for the pressure, but more stable oscillation. Due to turbulence being mainly a three-dimensional effect, in two-dimensional cases, vortex tubes are more robust and rolled up eddies survive longer than in three-dimensional cases. This fluid structures disturb cause the oscillations in the three-dimensional model to be weaker but more stable.

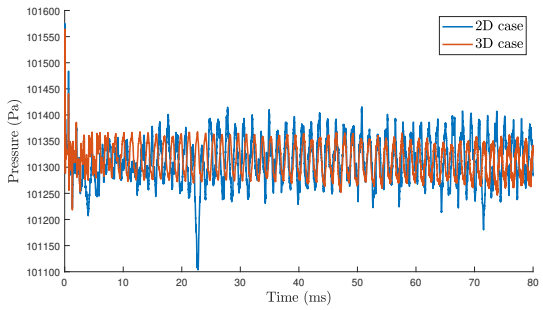


Figure 9

Due to the high computational cost of the three-dimensional simulation, only the last 28.7 ms of simulation were able to be used to calculate the far field acoustic data through the FWH acoustic analogy. Figure 10 shows the obtained results and plots them together with the experimental results of Fischer *et al.* [1]. Even with a visible difference in shape due to the difference on values taken, the FWH aeroacoustic analogy captures correctly the shape of the SPL, with the higher peak situated at the corresponding 700 Hz of the first harmonic, with the rest of the peaks greatly defined.

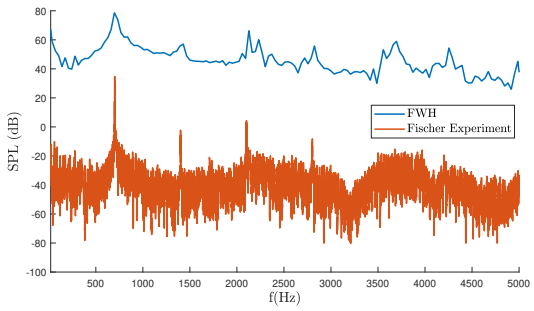


Figure 10

## 4. Conclusions

The main focus of this study was to simulate a three-dimensional model of an organ pipe. A LES turbulence model was employed and the FWH acoustic analogy was used to perform the aeroacoustic simulation.

To validate the computational strategy, first the noise induced by a squared cylinder was considered, The obtained results helped validating the methodology and understanding the behaviour of the acoustic field. The compressible and laminar simulation well reproduce the aerodynamic forces that cause the aeolian tones, as seen in Table 1, and the acoustic field, proven through the directivities plot in Figure 1.

Next, a two-dimensional model of an organ pipe is considered. The flow is modelled via LES and the results follow well the expected behaviour for the generation of sound, as seen in Figures 2 and 3. The acoustics have also a good representation on this model, obtained both directly from the flow field and through the FWH acoustic analogy. It was also proven that the obtained acoustic from the two-dimensional model behave correctly on changes of geometry.

Finally, the three-dimensional model shows similar results as the two-dimensional case. Differences are present due to the nature of the two-dimensional flow and the effects of turbulence. Regardless, the three-dimensional case is more stable and captures better the acoustics both through the flow field and through the FWH acoustic analogy. Nevertheless, the high computational cost of the three-dimensional simulation with respect the two-dimensional model do not compensate the quality of in the results.

The use of the FWH analogy is validated, getting the acoustic pressure outside the computational domain. Both in the two-dimensional an three-dimensional models, its use provides good understanding on both the harmonics and in the amplitude.

## References

[1] Jost Leonhardt Fischer, Rolf Bader, and Markus Abel. On the dynamics of the flow and the sound field of an organ pipes's mouth region. *arXiv: Fluid Dynamics*, 2019. doi: 10.48550/ARXIV.1912.06484. URL `https://arxiv.org/abs/1912.06484`.

[2] Akira Yoshizawa. Statistical theory for compressible turbulent shear flows, with the application to subgrid modeling. *The Physics of Fluids*, 29(7):2152–2164, 1986. doi: 10.1063/1.865552. URL `https://aip.scitation.org/doi/abs/10.1063/1.865552`.

[3] O. Inoue, M. Mori, and N. Hatakeyama. Aeolian tones radiated from flow past two square cylinders in tandem. *Physics of Fluids*, 18(4):046101, 2006. doi: 10.1063/1.2187446. URL `https://doi.org/10.1063/1.2187446`.